How technological advances in seismic acquisition, processing and imaging can bring new insights to near-field exploration

Federico Buriola[1]*, Jaswinder Mann-Kalil[1], Thomas Latter[1], Idar Kjørlaug[1] and Anna Rumyantseva[1]

demonstrate how dual-azimuth data and innovative processing and imaging technologies bring a significant imaging uplift over the Northern Viking Graben.

Introduction

The Northern Viking Graben (NVG) area of the Norwegian North Sea continues to be a focus of active oil and gas exploration. Recent exploration effort has created considerable value through several discoveries that will be tied into existing production and transportation infrastructure (commonly known as near-field exploration). The Resource Accounts for the Norwegian Continental Shelf, as per 31 December 2022, published by the Norwegian Petroleum Directorate (NPD, 2023) shows that exploration activity in the NVG area has led to the discovery of more resources than the rest of the Norwegian North Sea in eight of the last ten years. The technical success ratio of wildcat wells, as defined by the NPD, has been on average 47% per year within the NVG area compared to 30% outside it. These discoveries have been made in a variety of play types such as the injectite sand play in the Kveikje (35/10-8S), the Lower Cretaceous submarine deposits in Hamlet (35/9-16S), the Upper Jurassic submarine deposits in Swisher (35/11-24) and the classic rotated Middle Jurassic fault blocks in Toppand (35/10-7S). Exploration for these new and established plays requires regional insight, plus a local understanding of small-scale variations that are reliant on ever-improving seismic data.

The NVG area is covered by a BroadSeis™/BroadSource™ 3D seismic survey, extending over 44,000 km^2, that CGG acquired between 2014 and 2018 in a north-south acquisition direction and most recently re-processed in 2018 (referred to here as the 'legacy' data). This dataset contributed to many discoveries, providing a solution to the previous lack of regional high-quality seismic coverage in the area. However, the increasing focus on near-field (i.e. infrastructure-led) exploration demands data with improved imaging, resolution and signal-to noise ratio (SNR). The decision was therefore taken to initiate a new multi-year acquisition programme (from 2020 to the present) to acquire east-west triple-source multi-sensor seismic data over a 24,000 km^2 area, adding a second azimuth to the existing north-south survey (Figure 1). We demonstrate how, by combining the two azimuths in a contemporary dual-azimuth (DAZ) imaging sequence using the latest technologies in signal processing, DAZ visco-acoustic full-waveform inversion (FWI) velocity model building and imaging, we can address these demands. Leveraging the two datasets in conjunction with the latest imaging technologies, is shown to produce significant imaging uplift over the single-azimuth (SAZ) legacy data in terms of improved illumination, structural imaging, resolution and SNR.

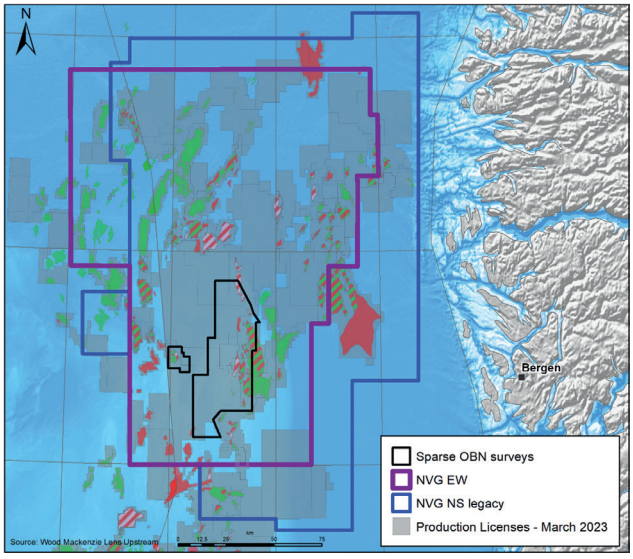

Figure 1 Location map showing CGG's legacy north-south and new east-west seismic data coverage, and sparse OBN layout in the Northern Viking Graben area.

Technology overview – Acquisition

North-south single-azimuth data were acquired with a dual source, a natural bin size of 6.25 m x 18.75 m and variable-depth 8km-long streamers towed at a depth of 7 m at near offsets and reaching a depth of 50 m in the second half of the cable (Soubaras, 2010). This configuration provided low-frequency fidelity, which is key for imaging resolution, notch diversity over the full bandwidth to compensate for the recording of receiver ghosts, and for the stability of FWI.

New east-west data were acquired with a triple source for denser spatial sampling (6.25 m x 12.5 m), an 8-km maximum offset with 18-km flat-tow and multi-sensor streamers, meaning

[1] CGG
* Corresponding author, E-mail: Federico.buriola@cgg.com
DOI: 10.3997/1365-2397.fb2023036

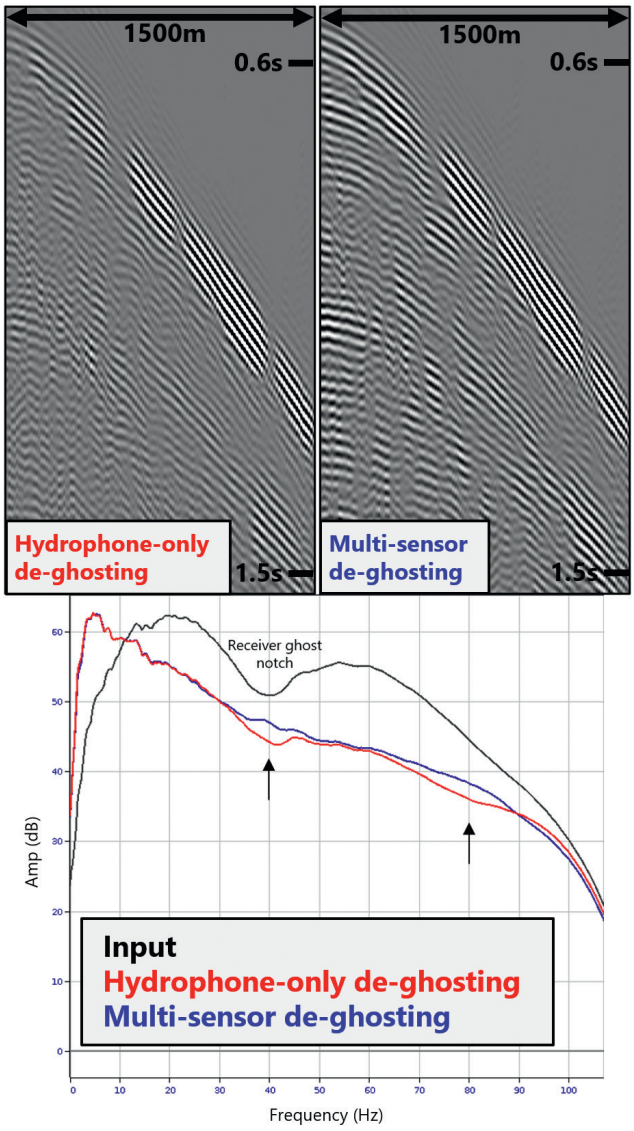

Figure 2 Comparison between hydrophone-only and multi-sensor receiver de-ghosting for east-west data on amplitude spectra (bottom) and on a shot gather filtered between 40 Hz and 50 Hz (top). Multi-sensor de-ghosting allows for improved signal recovery at around 40 Hz and 80 Hz compared to hydrophone-only de-ghosting, due to the contribution of accelerometer information.

accelerometer components were recorded in addition to the hydrophone recording. Being orientated perpendicular to the original data, the east-west data provide complementary illumination to the original north-south acquisition, increasing the recording aperture. This improves the illumination and amplitude fidelity of many structural elements in the area, particularly those with rugosity at and below the Base Cretaceous Unconformity (BCU) and, more generally, beneath the overburden complexity. SAZ recording aperture limitations also indicate wavefront noise ('smiles') due to non-cancellation of energy during migration. As this noise, along with more common coherent and random noise, is not repeatable between the two surveys, both azimuths can be leveraged to attenuate the unwanted energy and improve the SNR.

Variable-depth streamers rely on notch diversity and inversion-based receiver de-ghosting techniques to compensate for receiver ghosts and recover the full bandwidth. Multi-sensor cables, on the other hand, exploit the directivity of the receiver ghost, as constructive ghost interference in the accelerometer corresponds to destructive interference in the hydrophone notch, and vice versa. This increased signal recovery and SNR, particularly at mid frequencies, facilitated improved resolution compared to hydrophone-only de-ghosting (Figure 2). On the other hand, the deeper tow for the north-south data results in more low-frequency energy compared to the east-west multi-sensor data below 7 Hz (Latter et al., 2022). This means that the two azimuths have unique spectral content benefits, in addition to their complementary illumination and noise variations.

Technology overview – Pre-processing

Ongoing advances in processing and imaging technology and compute power motivated the decision to re-process existing regional north-south data, in parallel with the processing of the newly acquired east-west data. This section describes the combined processing of the two azimuths and key signal processing technologies that contributed to a significant imaging uplift over the legacy data, initially described over a subset of the regional area by Latter et al. (2022).

The de-signature flow was updated to include an iteratively reweighted sparse 3D joint source and receiver de-ghosting inversion. This updated flow firstly facilitated improved attenuation of out-of-plane ghost energy, which is important for imaging complex structures such as injectites and faults. Secondly, it considered 3D source array effects, reducing the residual ghost on outer cables. Lastly, by inverting for both source and receiver ghosts simultaneously, it made enhanced signal recovery at low frequencies possible, aiding resolution and the suitability of the data for inversion. For the east-west multi-sensor data, the inversion was extended to include accelerometer information and data-domain sparseness weights to improve the usable bandwidth of the data (Poole and Cooper, 2018).

Multiples are a particular challenge over the NVG area owing to the complex near-surface geology and a rugose Jurassic stratigraphy. Furthermore, the NVG area is located in shallow water, so many convolutional methods, such as Surface Related Multiple Elimination (SRME), can struggle to accurately predict multiples because of inadequate recording of the shallow multiple generators. In this scenario, 3D multi-channel deconvolution imaging and wavefield extrapolation-based de-multiple (Poole, 2019) helped to model multiples with greater accuracy and attenuate residual multiples observed in the legacy data. Novel approaches were also implemented to deal with challenging residuals, such as sub-BCU diffracted multiples. These included image-domain adaption and demigration of the adapted models. Such methods, with seamless transposition between data and image domains, were feasible over the regional surveys only as a result of advances in technology and compute power.

Several novel de-noise techniques were implemented throughout the processing sequence to increase the SNR and resolution. As an example, Figure 3a and Figure 3b show the application of a guided de-noise approach (Song and Messud, 2021) based on a Deep Convolutional Neural Network (DCNN). The process was instrumental for removing middle- to high-frequency noise, which otherwise could have degraded the imaging of thin-layered structures and the continuity of events. Co-operative denoise was

also performed between the surveys, extending the DAZ benefits beyond illumination and sampling enhancements. Co-operative denoise was particularly effective at removing coherent wavefront noise along the BCU, which can otherwise obscure fault interpretation as shown in Figure 3c and Figure 3d, which compare SAZ data and the new DAZ data. The DAZ combination processing also included octave-split DAZ stacking, aided by cross-correlation weights (Hung and Yin, 2012), to ensure illumination differences were optimally leveraged. Cumulatively, the signal processing developments in the DAZ combination processing flow were pivotal in achieving the overall uplift in the data shown in Figure 11 (from Latter et al., 2022), in combination with the higher resolution and higher-fidelity imaging velocities discussed in the next section.

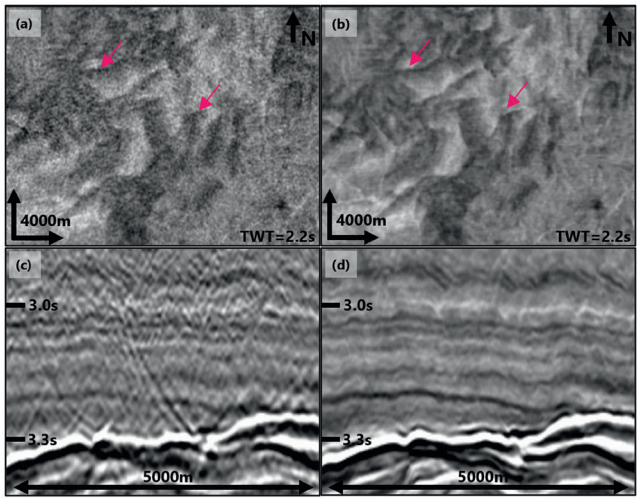

Figure 3 Time slice of full stack before (a) and after DCNN denoise (b), showing removal of high-frequency noise masking fault imaging. (c) Full stack of legacy data and (d) new DAZ data, highlighting the wavefront noise removal at BCU due to DAZ co-operative denoise.

Technology overview – Velocity model building

The legacy regional velocity model, covering an area of 44,000 km^2, was built in 2018 using north-south data and the latest advanced technologies available at that time, including multi-layer RMO tomography, least-squares diving-wave FWI up to 8 Hz and Q-FWI (Xiao et al., 2018). The legacy model was smoothed as a starting point for generating new DAZ velocity and attenuation (Q) models. DAZ Q-FWI above the maximum depth of penetration of diving waves was followed by DAZ Time-lag FWI (TLFWI, Zhang et al., 2018) up to 12 Hz. TLFWI utilises the full recorded wavefield, including diving waves, ghosts, multiples and primary energy, to invert for high-frequency details at deeper depths, including sub-BCU targets. Finally, long-wavelength updates were performed through DAZ multi-layer RMO tomography. Figure 4 shows the level of spatial and vertical resolution obtained with the new DAZ model, along with greater conformability to the underlying geology. Localised high-velocity anomalies were better captured in the presence of injectites and mounds as shown by the arrows; this was crucial for improved focusing, and resolving non-hyperbolic moveout and imaging distortions of the layers beneath. Improved matching to well logs was also observed across the whole survey, with the main velocity inversions at Top Rogaland and BCU better resolved.

To derive a new high-resolution Q field which accounts for amplitude attenuation and phase dispersion, we took a multi-

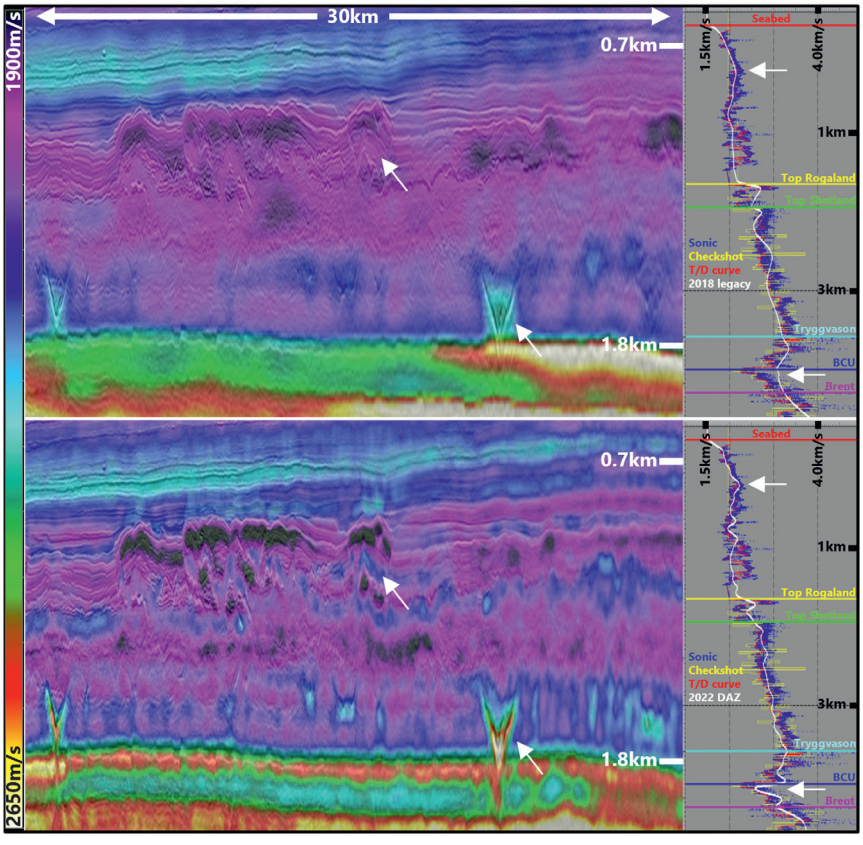

Figure 4 Velocity model – (top) 2018 legacy model with velocity profile overlain on the sonic log and check shot and (bottom) equivalent for the new 2022 DAZ model. The new model shows improved lateral and vertical resolution.

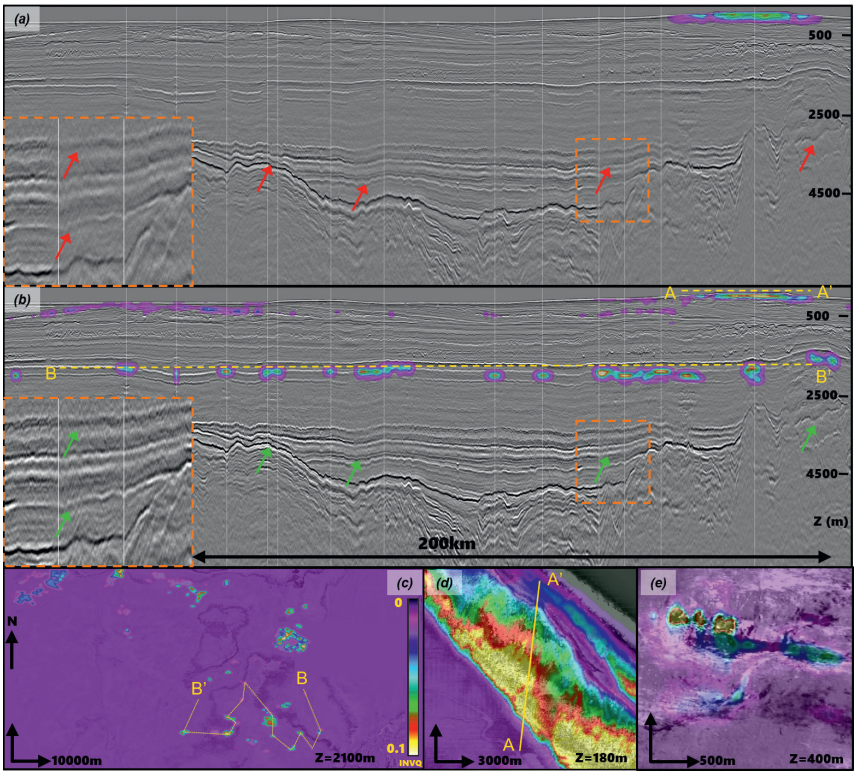

Figure 5 (a) East-west data Q-PSDM fence image of legacy Q model and (b) new DAZ Q models. (c) Deep depth slice through new Q model, along with shallower depth slices in (d) and (e). Note on the vertical cross-sections, inverse Q values beneath 0.01 are set to transparent to highlight localised bodies. From Latter et al. (2023).

process approach. This included: DAZ Q-FWI for the shallower sections where diving wave illumination was more complete; DAZ TLFWI-guided ray-based Q-tomography to resolve deeper Q bodies with high resolution; and synthetic validations using Q-sensitive metrics to fine-tune the background Q field (Latter et al., 2023). This Q model was honoured in the data modelling for the later TLFWI velocity inversions to ensure more accurate inversion convergence owing to reduced multi-parameter cross-talk. Compared to the legacy model (Figure 5a), the final DAZ Q model (Figure 5b-Figure 5e) showed higher resolution just below the seabed (Figure 5d-Figure 5e) with better delineation of the isolated shallow gas features, as well as accurate inversion for deeper attenuation sources missing in the legacy model, such as larger multi-level gas systems. Q-PSDM using the higher resolution and fidelity velocity and Q models (Figure 5b) showed improved spatially variable compensation of phase dispersion and amplitude attenuation, as well as improved structural continuity and amplitude balancing.

Ninety five wells spread across the entire area were used to help constrain the velocity and anisotropy parameters. The final mis-ties of the new model to geological tops were reduced for all main events compared to legacy, particularly for sub-BCU horizons. For instance, the absolute average and percentage mis-ties were decreased from 50 m (1.62 %) to 12.79 m (0.41 %) for the Top Brent layer, demonstrating that the new DAZ velocity model had a significantly improved depth registration.

Interpretation

As previously described, several factors contributed to the significant uplift in structural imaging provided by the new DAZ data including illumination enhancement from the second azimuth (Figure 11, from Latter et al., 2022). The improved imaging of faults on the DAZ volume was also validated by a machine learning-based fault-picking method, which shows how the picking on the new data is characterised by greater continuity and a reduced number of false positives (predicted but non-existent faults) when compared to the legacy data (Figure 11c and Figure 11f). Interpreting the data further, the increased resolution, structural imaging and SNR afforded by the new DAZ data provide further detail and greater interpretability to thin-bed evaluation of reservoirs. During recent years, exploration activity in the northern part of NVG has targeted the Dunlin Group (Gp) and particularly the Cook Formation (Fm), resulting in the discovery of hydrocarbons in the Knarr Field, Garantiana Field and Garantiana satellites. At Knarr and Garantiana, the Cook Fm consists of up to five sandy reservoir levels (Skarpeid et al, 2018). Imaging of these levels is crucial to deriving the potential volume of a prospect and discovery and for reservoir model building. Figure 6 shows an east-west oriented line going through Well 34/6-1S, intersecting three different Cook Fm sandstones highlighted in yellow by the gamma ray log. The new DAZ dataset (Figure 6b) allows for a stronger tie between the thin layers within the Cook Fm and the gamma ray log while the corresponding SAZ legacy data (Figure 6a) maps the events with less confidence. The three Cook Fm sandstones are also captured by TLFWI as three different low-velocity layers in the new DAZ velocity model (Figure 6d, in green), which are not observed in the lower-resolution legacy model (Figure 6c). This opens up the opportunity of using the new high-resolution velocity model as an attribute in the reservoir evaluation.

The new DAZ data provide not only improved analysis of thin-layer structures but also improved interpretation of regional-scale depositional systems like the Upper Jurassic

Intra-Heather Formation sands (Sognefjord Fm, Fensfjord Fm and equivalents). Wells targeting these sands have resulted in many recent discoveries such as Swisher (2020) and Blasto (2021). By using the new DAZ data, it is possible to conduct detailed evaluation of sediment depositional pathways and potential reservoir characterisation through spectral decomposition using a red-green-blue (RGB) colour blending model (Mann-Kalil, 2023). This is an effective way of displaying the responses between different frequency bands, as shown on a horizon extraction within the Late Jurassic sequence over the Horda Platform (Figure 7a). Here we can identify bright amplitude anomalies representing multiple routing systems feeding sediment into the basin along incised canyon systems and splaying out into lobe complexes. The horizon was determined from the DAZ data using an automated extraction across a window from the BCU down to the Top Statfjord Fm. This automatic process was difficult to conduct when interpreting the legacy data, owing to the lack of continuous reflectivity and the presence of noise. The automated process has been improved with the DAZ data due to better crossline sampling, demultiple and denoise processes (Figure 7b and **7**c).

Seismic inversion studies are beneficial for mapping the probabilities of different lithofacies, fluid classifications and porosity estimations, as well as for investigating uncertainties at the well locations. Here we show results from an elastic inversion study conducted over the Tampen Spur area, in a deliberately chosen location where azimuthal imaging variability was small between north-south and east-west data on full angle stacks (Figure 8c and Figure 8d). However, it is worth emphasising that the full stack is the least sensitive way of viewing the data. Azimuthal amplitude changes in areas that were similar on full stacks were still shown to have a profound impact across angles as shown on common image gathers (CIG) below 3000 ms (Figure 8a and Figure 8b). Considering that we expect similar rock physics responses

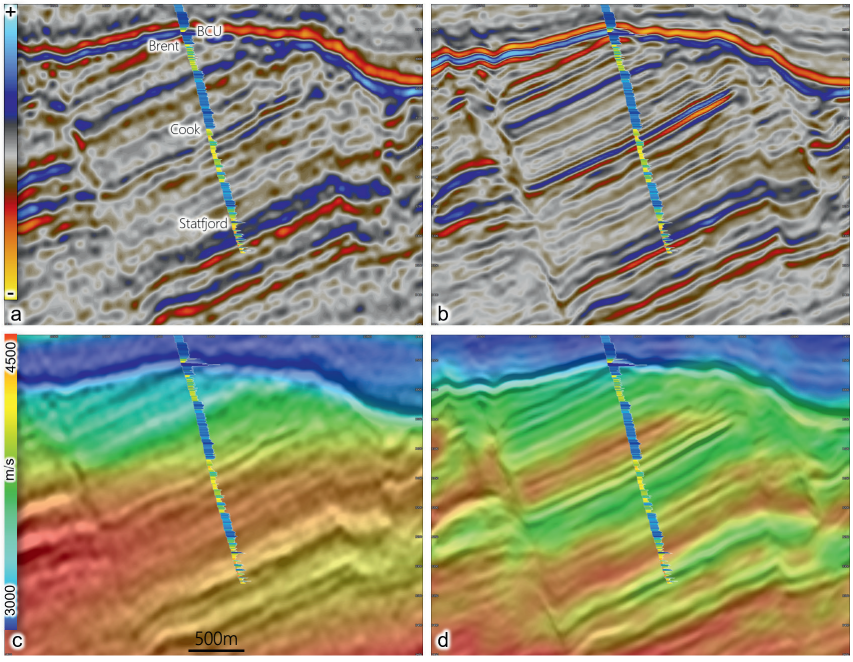

Figure 6 An east-west section through Well 34/6-1S. (a) Legacy full stack and (c) velocity model. (b) DAZ full stack and (d) new DAZ velocity model. The gamma ray log shows the presence of sandy intervals marked in yellow.

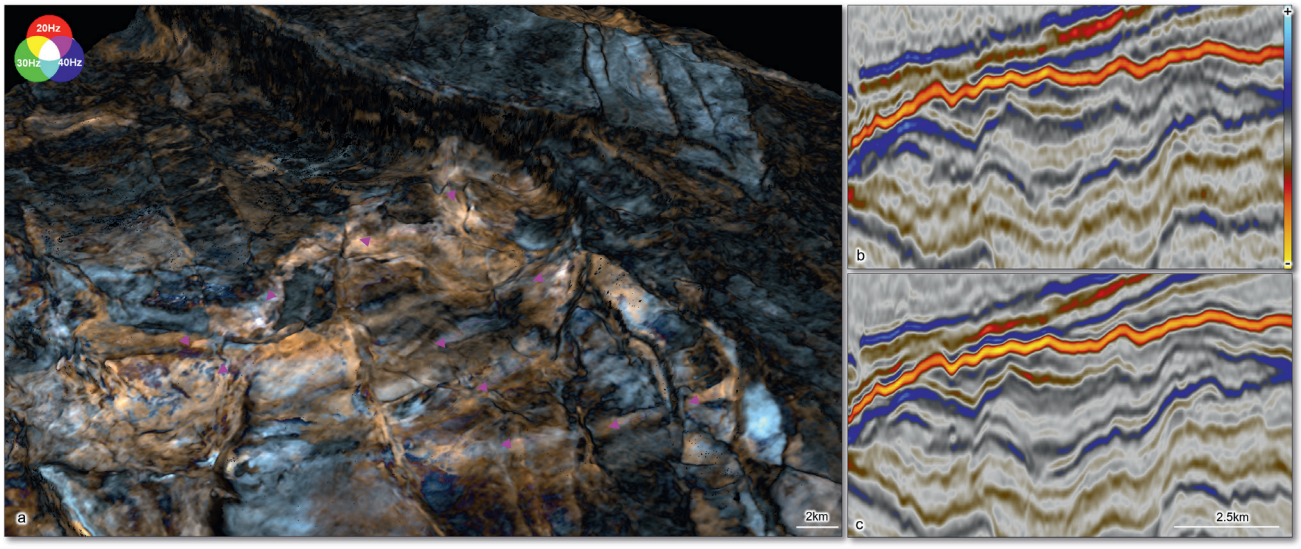

Figure 7 (a) Spectral decomposition RGB-blend of a Late Jurassic surface showing sediment routing systems (magenta arrows). (b) Legacy full stack. (c) DAZ full stack.

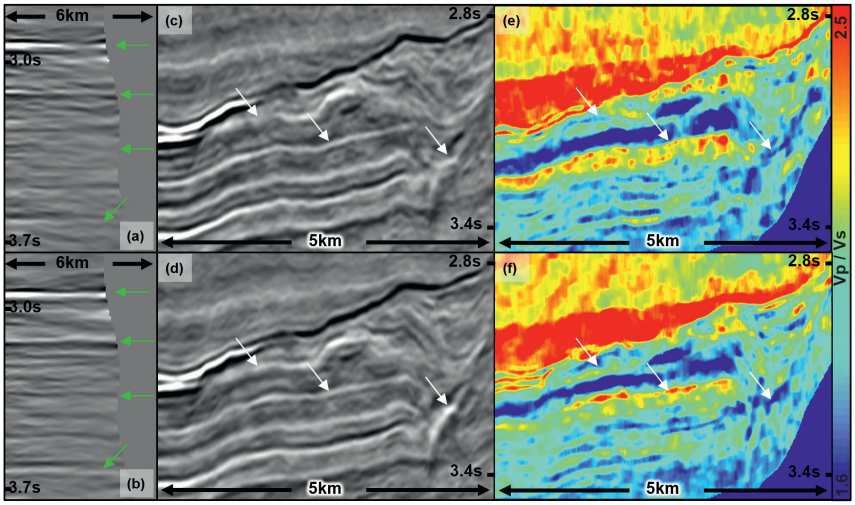

Figure 8 North-south (a) re-processed gather, (c) full stack and (e) estimated Vp/Vs ratio. (b, d, f) Equivalent for east-west. Even in areas where structural imaging on full stack is comparable between two azimuths, local variations in AVO and Vp/Vs ratio are visible as highlighted by the arrows.

between the azimuths and the consistency of the processing and imaging sequences, we attributed this primarily to azimuthally variant illumination affecting amplitude fidelity. It is worth mentioning that subsurface azimuthal variability within each 2D CIG may influence this assumption, notably on the near offsets. However, this effect is expected to be small, below 3000 ms. Vp/Vs results in Figure 8e and Figure 8f show how the AVO response is subject to local variations between the two azimuths even where the structural imaging may be similar. Thus, the DAZ data provide a broader perspective for reservoir characterisation and greater potential for de-risking beyond what could be achieved with SAZ data alone.

We can start to evaluate inversion results in relation to reservoir targets through P-impedance estimates and probability of sands (Figure 9, Mann-Kalil et al., 2023). We see the results in the Late Jurassic sequence, where a combination of slumped and canyon-driven deposits lie above the Brent Gp. A strong correlation can be established between the P-impedance response (Figure 9a) from the well (blue), the response extracted from the north-south data (green) and the response extracted from the east-west data (red). Late Jurassic slumped deposits, resulting from gravitational collapse at the Snorre structural high, are identified as a dense high-impedance body when the P-impedance is superimposed on the DAZ seismic section (Figure 9b). In contrast, the hemipelagic and canyon-fed deposits show a low-impedance response, conforming to the characteristics of these different bodies observed in the data. A facies classification process was also performed as part of the elastic inversion. Lithology and fluid classifications were trained and run using petrophysical-driven lithologs, Backus averaged in-situ logs, P-impedance, and Vp/Vs inversion results. Figure 9c and Figure 9d show north-south and east-west seismic sections, respectively, superimposed with the probability of sand, coloured in yellow. The probability of sand correlates with confidence to the gamma ray log at Well A, highlighting the presence of sand-rich layers in the Late Jurassic sequence shown by both azimuths. Here is an example of the difference in detail seen in azimuthal variations and the benefits of having a denser amount of data to work with. The result demonstrates the importance of analysing multiple data sets, honouring all data and incorporating the results into the range of outcomes in an evaluation.

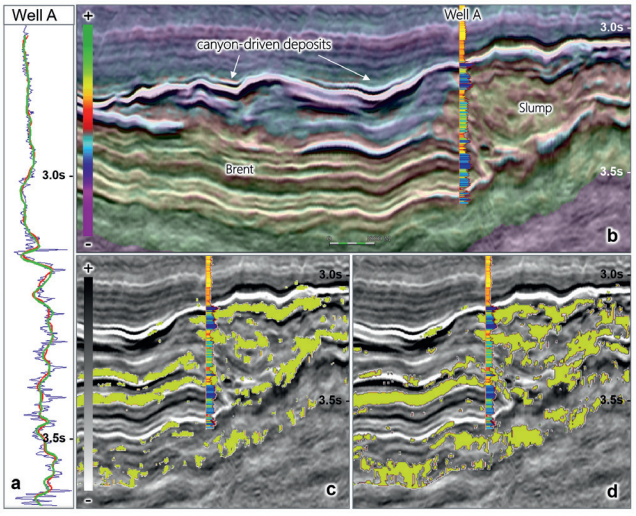

Figure 9 (a) P-impedance curve from Well A shown in blue, P-impedance curve extracted from inverted east-west data in red and north-south in green. (b) DAZ full stack overlain with estimated P-impedance. (c) North-south full stack overlain with probability of sand extracted from the same volume and (d) equivalent for east-west data.

What's next? OBN

While adding the second azimuth provided enhanced illumination, SNR and sampling, richer information can be recorded with ocean bottom nodes (OBN). OBN is the natural extension to DAZ data as it allows for: deeper diving wave penetration due to the potential to record longer offsets; full azimuthal information for further improved illumination, AVO and inversion reliability; the recording of converted waves; and improved signal recovery in hydrophone notches for increased resolution due to geophone recording, notably on the very low frequencies where surface seismic data can suffer.

This section illustrates initial results from a towed-streamer and node hybrid acquisition completed west of the Fram area, combining the DAZ streamer data, described earlier, with nodes (300 m x 300 m) that provide full-azimuthal recordings and longer offsets of up to 24 km. Diving-wave analysis demonstrated that the maximum penetration depth of diving waves is increased from 2 km to 4.5 km depth when the maximum offset is increased from 8 km to 24 km. As a result, low wavenumber

updates with FWI using diving waves produced a more stable velocity model in the deeper sections. The benefits of the long-offset and full-azimuth information from node data can be combined with the denser lateral sampling provided by streamer data, as demonstrated by the result of a joint TLFWI up to 30 Hz (Figure 10). Compared to the legacy, the new model provided a more accurate and higher-resolution velocity field at all depths. In addition, with long recorded offsets, the expected elastic effects induced by the large impedance contrast at BCU level can be inverted for by applying elastic TLFWI, to further improve model fidelity down to sub-BCU targets (Masclet and Wang, 2023).

Conclusion

The regional SAZ legacy data over the NVG area was processed as recently as 2018 and contributed to many discoveries. However, the continuing demand for de-risking near-field exploration requires data with improved imaging. With this objective, a triple-source multi-sensor survey recorded in the perpendicular direction to the legacy azimuth was acquired and processed, at the same time as the north-south data was re-processed. This produced new DAZ data which showed a significant uplift over the SAZ legacy in terms of structural imaging, illumination, resolution and SNR (Figure 11, from Latter et al., 2022). Factors contributing to the uplift can be summarised into four main categories: 1. illumination enhancement and denser sampling from the second azimuth; 2. advanced DAZ co-processing methods; 3. application of our latest processing technologies for de-signature, de-multiple and de-noise; 4. imaging using higher-resolution DAZ velocity and Q models, including our advanced TLFWI. This new dataset provided better definition of shallow targets such as injectites (Figure 11a and Figure 11d)

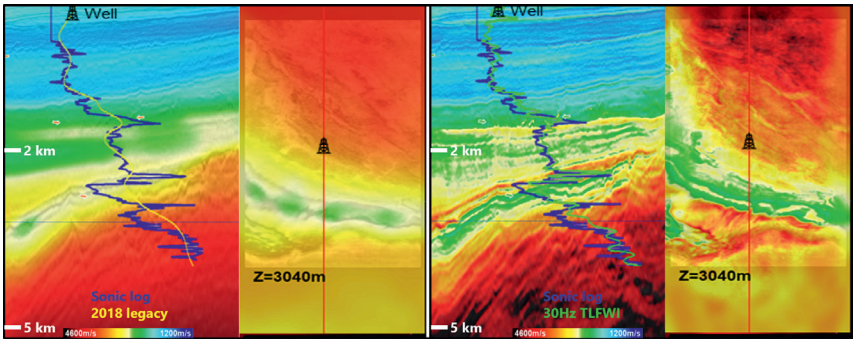

Figure 10 (left) Comparison of 2018 legacy model (section with velocity profile overlain on the sonic log and depth slide view) and (right) 30 Hz joint node and streamer TLFWI velocity model. From Masclet and Wang (2023).

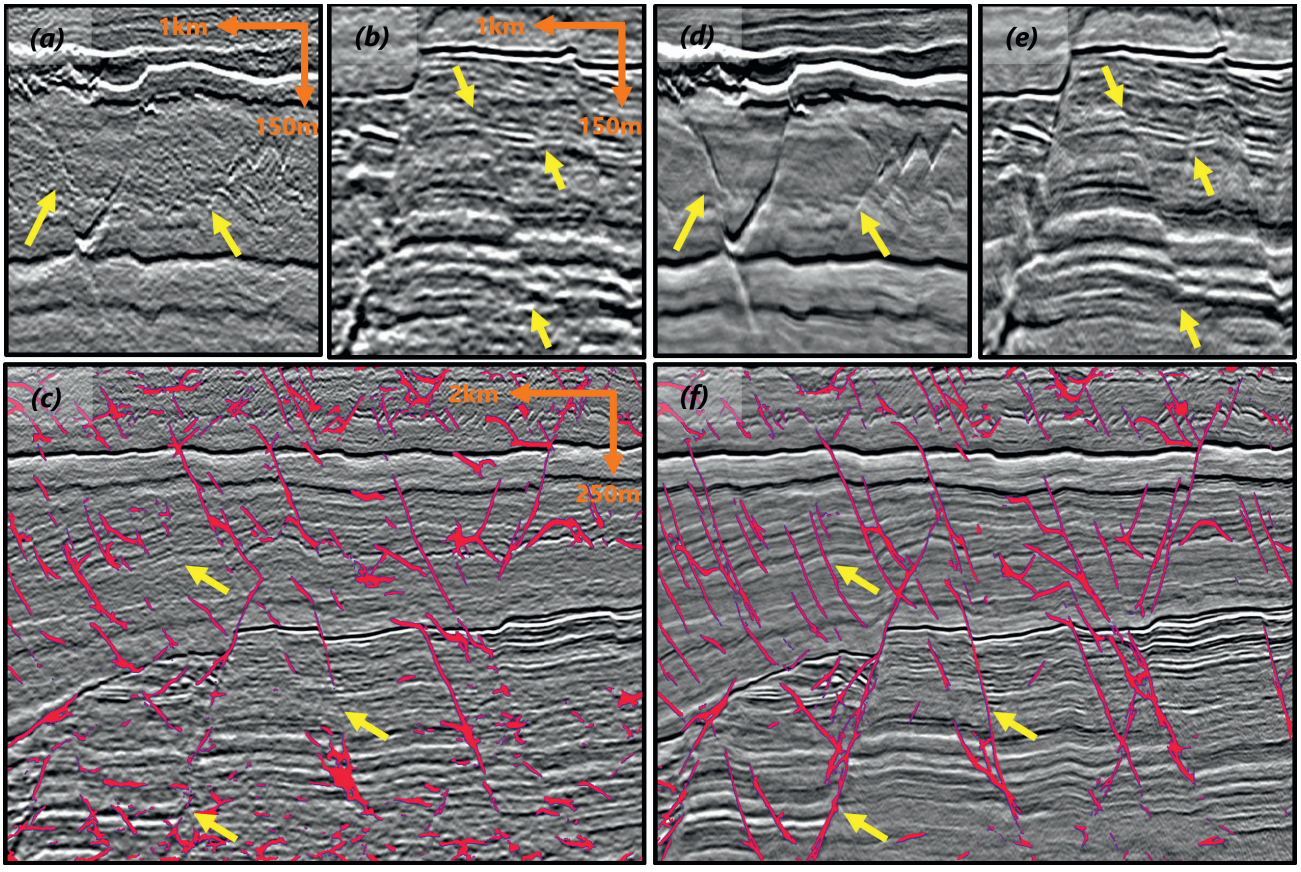

Figure 11 (a)-(c) Legacy north-south Q-PSDM full stack. (d)-(f) New DAZ full stack. Yellow arrows highlight clear areas of improved fault or injectite imaging. Images (c) and (f) show results of machine learning-based fault picking (in red) (from Latter et al., 2022).

and more confidence in the interpretation and mapping of deeper structures such as faults (Figure 11b and Figure 11e), the thin layering within the Cook Fm, and the sub-marine sediment routing systems within the Late Jurassic sequence. Furthermore, improved interpretability was confirmed by results from the machine learning-based fault picking (Figure 11c and Figure 11f), with faults picked with greater reliability in the new DAZ data. The improved amplitude fidelity with the addition of the second azimuth also provided new insights for seismic inversion studies. Even areas of similarity between the two azimuths in terms of structural imaging showed significant illumination differences across angles, providing additional information around AVO. Looking ahead, the imaging benefits of DAZ can be further extended with OBN data, where even better data will be able to take subsurface understanding further in the future. Finally, additional imaging uplift can be achieved with FWI imaging (Zhang et al., 2020) due to the least-squares data fitting methodology in the inversion process and full-wavefield sampling (including primaries, multiples, ghosts and diving waves). This is further explained over a sub-area within the NVG region by Dinh et al. (2023).

Acknowledgements

The authors thank their colleagues in the CGG Subsurface Imaging team for their contribution to the data processing and imaging results and CGG Earth Data for permission to publish the data examples.

References

Hung, B. and Yin, Y. [2012]. Optimal stacking for multi-azimuth pre-stack seismic data. *22nd ASEG Conference and Exhibition, Extended Abstracts*, 1-4.

Hung, D., Latter, T., Townsend, M. and Grinde, N. [2023]. *Dual-azimuth FWI Imaging and its potential in shallow hazard assessment.* 84th EAGE Annual conference & exhibition.

Latter, T., Gram-Jensen, M., Buriola, F., Dinh, H., Faggetter, M., Jupp, R., Townsend, M., Grinde, N., Machieu, C. and Byerley, G. [2022]. The value of dual-azimuth acquisition: imaging, inversion and development over the Dugong area. *83rd EAGE Annual conference & exhibition*, *Expanded Abstracts*.

Latter, T., Nielsen, KM., Beech, A. and Cantu Bendeck, D. [2023]. *Deriving a high-resolution regional scale Q model over the Northern Viking Graben*. 84th EAGE Annual conference & exhibition.

Mann-Kalil, J. [2023] *Enhanced regional imaging of Late Jurassic depositional systems across the Northern Viking Graben, Norwegian North Sea*. 84th EAGE Annual conference & exhibition.

Mann-Kalil, J., Rumyantseva, A. and Kjørlaug, I. [2023]. Northern Viking Graben – Chasing the Late Jurassic Play. *GeoExPro 2023*, Issue 2.

Masclet, S. and Wang, F. [2023]. *Hybrid Streamer Node acquisition: Unlocking sub-BCU targets with Elastic and High-Resolution FWI.* 84th EAGE Annual conference & exhibition.

NPD [2023]. Resources Accounts for the Norwegian Shelf as per 31.12.2022. https://www.npd.no/globalassets/1-npd/publikasjoner/rapporter/ressursregnskap/2022/resource-accounts-2022.pdf.

Poole, G. [2019]. Shallow water surface related multiple attenuation using multi-sailline 3D deconvolution imaging. *81st EAGE Conference and Exhibition*, *Extended abstracts*, Tu R01 05.

Poole, G. and Cooper, J. [2018]. Multi-sensor receiver deghosting using data domain sparseness weights. *80th EAGE Conference and Exhibition*, *Extended Abstracts*, We A10 08.

Skarpeid, S.S., Churchill, J.M., Hilton, J.P.J., Izatt, C.N. and Poole, M.T. [2018]. The Knarr Field: a new development at the northern edge of the North Sea. *Petroleum Geology Conference Series*, **8**, 445-454.

Song, H. and Messud, J. [2021]. Machine learning for seismic processing: The path to fulfilling promises. *91st SEG Annual Meeting*, *Expanded Abstracts*, 3204-3208.

Soubaras, R. [2010]. Deghosting by joint deconvolution of a migration and a mirror migration. *80th SEG Annual Meeting, Expanded Abstracts,* **29**, 3406-3410.

Xiao, B., Ratcliffe, A., Latter, T., Xie, Y. and Wang, M. [2018]. Inverting near-surface absorption bodies with full-waveform inversion: a case study from the North Viking Graben in the Northern North Sea. *80th EAGE Conference & Exhibition, Extended abstracts*, Tu A12 03.

Zhang, Z., Mei, J., Lin, F., Huang, R. and Wang, P. [2018]. Correcting for salt misinterpretation with full-waveform inversion. *88th SEG Annual International Meeting*, Expanded Abstracts, 1143-1147.

Zhang, Z., Wu, Z., Wei, Z., Mei, J., Huang, R. and Wang, P. [2020]. Full-wavefield imaging through full-waveform inversion. *90th SEG Annual International Meeting*, *Expanded Abstracts*, 656-660.